Body-centric Wireless Hospital Patient Monitoring Networks using Body-contoured Flexible Antennas

Philip A. Catherwood, Syed S. Bukhari, Gareth Watt, William G. Whittow, and James McLaughlin

DOI: 10.1049/iet-map.2017.0604 , Online ISSN 1751-8733

Body-centric Wireless Hospital Patient Monitoring Networks using Body-contoured Flexible Antennas

Philip A. Catherwood[1*], Syed S. Bukhari[2], Gareth Watt[3], William G. Whittow[2], and James McLaughlin[1]

[1] School of Engineering, Ulster University, Shore Road, Jordanstown, UK.
[2] School of Mechanical, Electrical & Manufacturing Engineering, Loughborough University, Leicestershire, UK
[3] Norbrook Laboratories Ltd, Newry, UK.
[*] p.catherwood@ulster.ac.uk

Abstract: This paper presents empirical results from a measurement campaign to investigate futuristic body-centric medical mesh networks for a hospitalized patient using flexible body-contouring antennas. It studies path loss in a medical environment (in a hospital bed in an open hospital ward) for UWB and four narrowband schemes concurrently. It firstly investigates the antenna contouring effects due to mounting the flexible antennas on various body surfaces, then uses statistical analysis to explore optimal body locations for a master node to inform allocation of processing power (assuming point-to-point link from other nodes). Results indicated how the most suitable body location varies depending on the posture and frequency scheme used. Also investigated are best route selections for multi-hop mesh network topologies for opportunistic networking for each of the presented postures and frequencies; this reveals how less hops were required to navigate around the narrowband network compared to UWB which effectively reduces required processing power and data traffic. Understanding how disparate body-centric medical devices communicate with one another in a body-mesh network is instrumental to the strategic and informed development of next generation healthcare patient monitoring solutions.

1. Introduction

Body-area networks (BAN) have attracted much attention in recent times due to the emerging wearables market [1], and medical BANs have been highlighted as a solution to deliver better healthcare, synchronous automated data collection, and intelligent diagnostics in busy clinical environments [2]. Such systems would monitor multiple biological indicators essential to timely diagnosis and evidence-driven interventions. This technology paves the way for new treatment strategies unachievable with current technologies. One key building block of such a medical BAN is the wireless links between wearable bio-sensor nodes. A number of different radio technologies have been advocated as suitable for BAN realization, including Ultra-wideband (UWB) [3-6] and narrowband [6-8] schemes.

It is also important to consider how patient posture may affect on-body data links in a hospital environment. Work by [3] reported how body geometry changes will change the channel impulse response. Investigations by [4-7] each presented path loss measurements in various environments between the master node (waist) and a range of distributed transceivers on several body areas (wrist, head, chest, ankle, thigh, hand, etc.). Of particular note, [5] studied the effects of sitting and standing positions on path loss. However, our paper specifically studies narrowband and UWB path loss for a bed-bound subject in a medical environment, and only [8] has presented results for a user lying in a bed at a single frequency of 2.4 GHz for point-to-point links between the user's wrist, waist, and ankle. Sensor positioning is also significant as the medical measurement dictates location. Example positions include the chest where electrocardiograms (ECG), respiration, arterial oxygen saturation (SpO_2), and Pulmonary Edema monitoring can be implemented [4, 9, 10, 11]; the waist for implanted glucometers; the wrists which are a future site for ECG [12]; the upper arm (bicep) area is a common place for blood pressure cuffs; and the ankle for ankle-brachial index measurements [13].

Much of the literature reports on medical BANs using a radial point-to-point topology with an off-body master node, typically some form of base station access point (e.g. bedside node) for the various wearable sensors [4-8]. A number have studied mesh networks [14-19] but have not specifically focused on medical scenarios at these frequencies, postures, and environment. Relaying schemes have been previously investigated; [16] investigating Packet Error Rate (PER), is based on measured time-variant channels at 2.45 GHz to improve the robustness of the communication between two on-body nodes, [17] who analysed routing and network architectures for indoor walking scenarios at 2.45 GHz, [18] who investigated opportunistic relaying protocols for 2.45GHz real time to common sink wearable networks for walking scenarios, and [19] who showed that multi-hop networking minimises retransmissions as well as having better network lifetime and lower delay and energy consumption at 2.45 GHz.

The presented work investigates which medical sensor location is the key processing node for point-to-point links from other nodes, and discusses the best route selection for multi-hop mesh network topologies. This helps identify the potentially busiest routes in such an opportunistic mesh network to best allocate processing power and avoid routing bottlenecks [20]. This work has applications for both emerging wireless vital-signs monitors and long term ubiquitous healthcare.

The use of mesh networking increases network complexity and cost, however it has a number of benefits

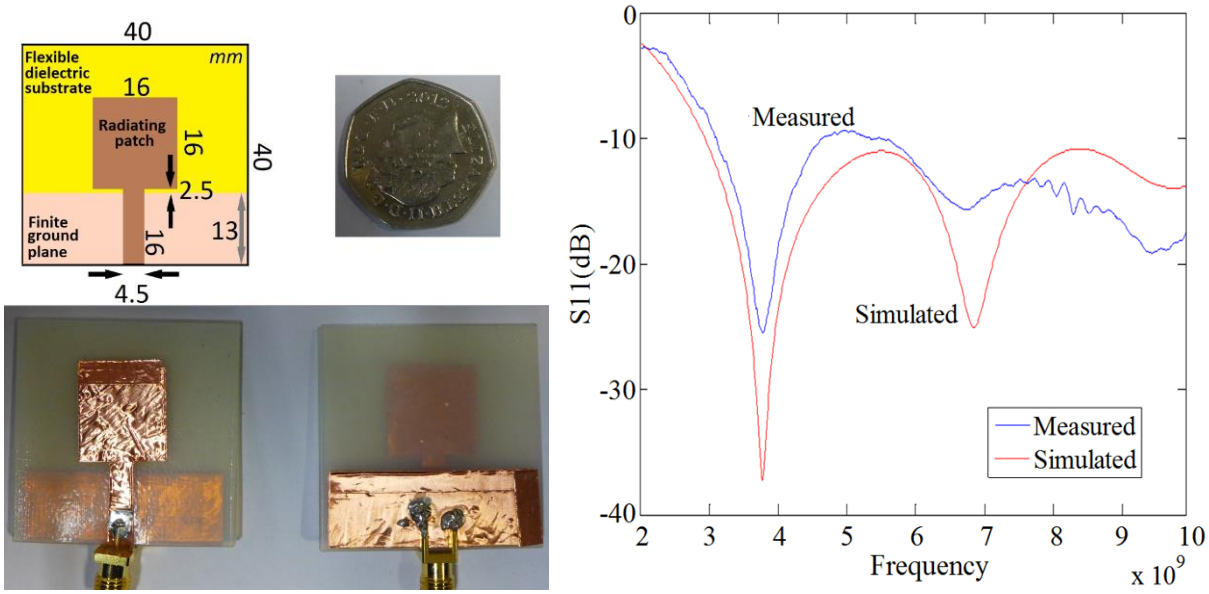

(a). ***(b).***

Fig. 1. *Rectangular patch antenna.*
a) Antennas with design geometry
b) Measured and simulated S_{11} results of antenna (CST Studio suite).

that are attractive for battery-powered real time fully synchronous whole-body bio monitors including strategies of edge and distributed computing, operation in unfavourable environments, and reliable performance under low transmission powers [14-19]. Such attributes are essential to usher in next generation healthcare technology.

Flexible antennas can be shaped to the contour of the body surface to which they are applied. Previous work has shown how bending flexible antennas affects radiation pattern [21] and resonant frequency [22]. The antennas used in this paper are UWB antennas; the performance effects of antenna bending are considered as part of the overall results. This study is focused in a hospital ward for the purpose of near-future deployment and has commercial impact as many companies deploy wireless medical systems without understanding the radio channel characteristics. This work presents for the first time a direct comparison between multiple frequencies in the UWB spectral band for a BAN using flexible antennas in a medical environment.

2. Experimental Arrangements

2.1. Measurement System

The wearable body-area network system comprised of an UWB bi-static radar system [23] specifically selected to allow the UWB frequencies and the four narrowband frequencies of interest to be captured simultaneously using a single piece of equipment. The battery-powered Time Domain PulsON210 source had a narrowband launch power of -12 dBm and path loss between nodes was recorded onto a laptop running Time Domain's bespoke software. The antennas (Fig. 1) were made from copper foil and a flexible 3D printed dielectric material (with a thickness of 2 mm). The compact printed microstrip-fed monopole antennas used were rectangular planar antennas which are popular for UWB applications and more suitable for body-worn applications than other antenna designs such as Conical, Log-periodic antenna, Spiral, etc. [24-25]. A rectangular radiating patch design was selected as it is easy to rapidly fabricate and tune, is considered an optimal choice for maximising on-body propagation [26], offers a suitable wide-bandwidth response at these frequencies, can be worn comfortably and potentially embedded into clothing [26], radiates omni-directionally with polarisation normal to the body surface, offers a base measurement for future bandwidth enhancement through more complex antenna geometry if desired, and explores the potential for using disposable sensors (including the radio chip and antenna) to address the ongoing issues of infection control in hospitals.

2.2. Measurement Environment

The measurement campaign was conducted in a 61 m^2 hospital ward (Fig. 2) with 6 beds. The building was of 1990's steel frame construction with concrete-block cavity external walls, single brick internal walls, and a concrete floor. A suspended ceiling supported fluorescent lighting at 2.6 m above floor level and the ward had double-glazed PVC-framed windows along one length of the room. The beds, bedside tables, and chairs were standard hospital supply. The environment in which an on-body network operates has been previously shown to have a marked effect on link performance at similar [27-28]; this investigation is presented in its typical operational environment of a hospital ward.

On-body radio channels are considered subject-specific [29] and on-body path loss for women is less than that for men [30]. Considering the finite-difference time-domain (FDTD) modeling results presented in [29] the difference in path loss at 2.45 GHz between a small slim female and a tall heavily-set male is notable for short-range links. However, the presented work focuses specifically on comparisons between the links as opposed to absolute values; as such it is recognized the body shape may still have an impact on the results but to a lesser degree. The measurements utilize a single-user as per [31-33], who was an adult male of mass

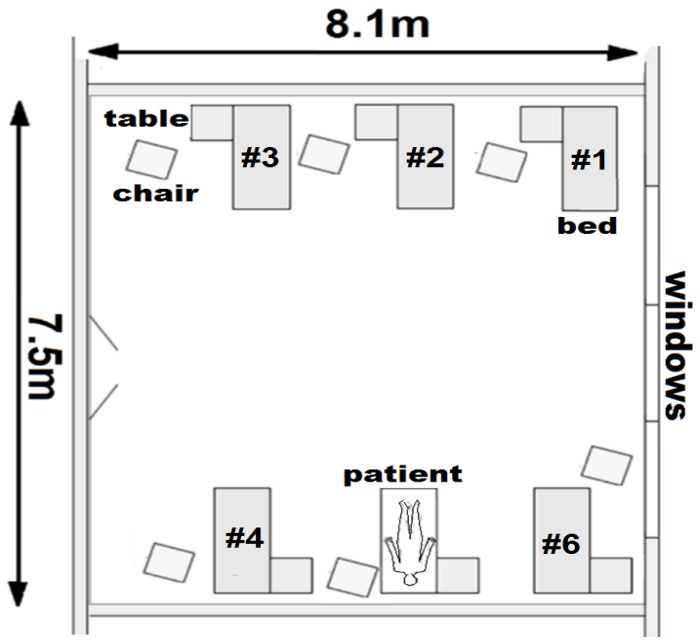

Fig. 2. *Test environment*
a) Hospital plan.
b)Photograph of hospital environment.

77 kg, height 1.73 m. Fig. 3 depicts the comparison between an isolated free-space antenna configuration (measured in an anechoic chamber) positioned on a wooden mount at a height of 1.4 m from the floor of the chamber and for a chest-mounted antenna (also at a height of 1.4 m from the floor of the chamber). As an example of the impact of placing the antenna on the body we present the UWB azimuthal radiation patterns for the above arrangements.

2.3. Procedure

Measurements were expressly taken for a stationary patient, as bed-bound patients typically make few movements and may remain immobile for some time in an intensive care unit. The patient was placed in two characteristic postures within the hospital bed; firstly lying down in the bed and secondly sitting up in the bed. These positions are particularly likely with the elderly in care homes and those undergoing observation in cases of serious illness, for example, following a cardiac event. The antennas were placed on various parts of the body (as depicted by green triangles in Fig. 6). A ten second sample was taken for each combination of transmitter/receiver location at 100 samples per second; samples were averaged to ensure each measurement was not biased by breathing movements and other instantaneous natural body fluctuations, with the measurement variations (± 3 standard deviations) of the sample sets for each frequency and posture (summarised in Fig. 8). Throughout testing the antennas were held in place by elasticated straps to eliminate antenna-body separation. Data was recorded to a laptop for UWB between 3.0 - 6.2 GHz and for narrowband frequencies of 3, 4, 5, and 6 GHz. A frequency domain technique was used during processing to remove the measurement system transfer function [23].

3. Results and Discussion

The wearable body-area network system comprised of an UWB bi-static radar system [23] specifically selected to allow the UWB frequencies and the four narrowband frequencies of interest to be captured simultaneously using a single piece of equipment. The battery-powered Time Domain PulsON210 source had a narrowband launch power of -12 dBm and the antennas were made from copper foil and flexible 3D printed material (Fig. 1).

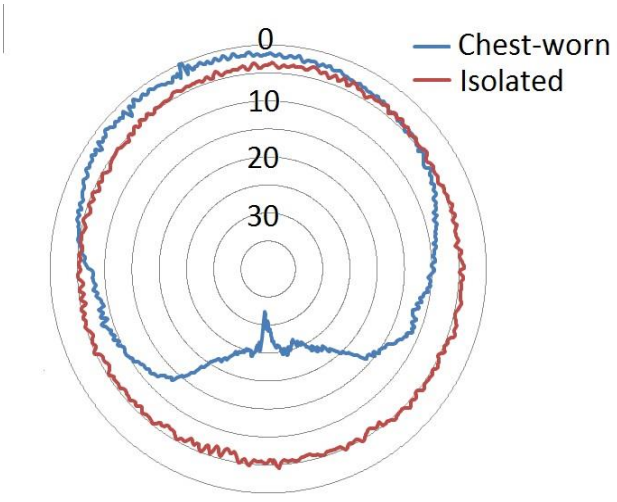

Fig. 3. *Azimuth UWB radiation pattern (Anechoic chamber) for isolated and chest worn*

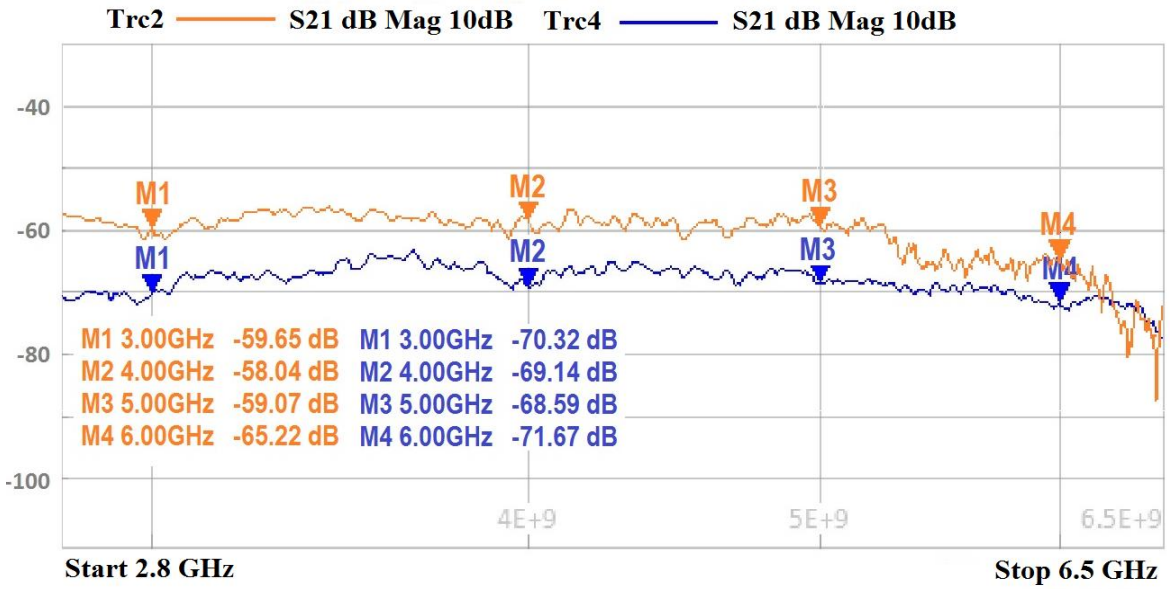

Fig. 4. *Frequency response (Orange trace (upper trace) waist to ankle lying down; Blue trace (lower trace) chest to waist lying down)*

Results are considered for the effects of contouring the antenna around the body (Table 1), firstly in the lying and sitting postures individually to investigate posture effects, then as a combined result (all data considered together and averaged accordingly) to examine the collective data for generalized scenarios. The combined situation attempts to understand channel properties for a patient wearing the system in either position; these are the two main positions for a bed-bound patient but a patient will be in both during the course of a day, so the combination of both positions offers useful insight. Many past measurements [4-7, 31-33] used the waist as the master node. While these did not specifically validate why the waist location was chosen its advantage can be inferred from the results, likewise the advantage of the chest is also expected from being mounted on the same surface. However, this advantage is not guaranteed for all frequencies and environments, hence this paper provides crucial insight regarding investigations for hospital environments where users are in bed wearing flexible body-contoured antennas.

Fig. 4 presents a representative example of the frequency response plots across the 3.0 - 6.2 GHz range (the band of experimentation and limitations of the measurement equipment). Every combination and permutation for all the nodes have not been presented to ensure suitable succinctness; as a principal example the main link (chest to waist) as well as a torso to extremity link (waist to left ankle) is presented. The figure illustrates how application to differing parts of the body create differing spectral responses in terms of link power and spectral response at each of the narrowband frequencies of interest, with any given sample measurement typically depicting a variation across the UWB of more than 10 dB**.**

3.1. Antenna Contouring Effects

The flexible antennas were contoured to the body surface to which they were applied; this inherently affects their designed performance [21-22]. To investigate the effects of the differing bend radius the antennas were curved to pre-determined radii for both the isolated case (Fig.5a) and for a body-mounted scenario (Fig.5b) on the torso to allow a comparison of the effects of the contouring and the

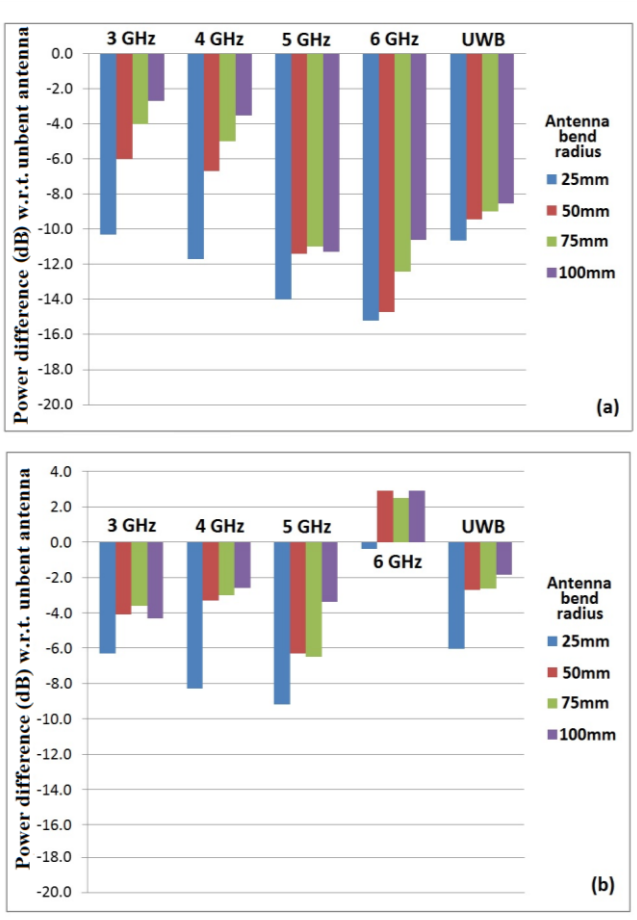

Fig. 5. *Link power for varying antenna curvature with respect to an unbent antenna*
a) Isolated antenna
b) body-mounted antenna

Table 1 Received power values (in dBm) for each permutation of test showing highest (_ _) and lowest (_ _) powers, and 6 standard deviation measurement variations (in dB) for each frequency and posture

		LYING					SITTING					COMBINED				
Tx	Rx	3GHz	4GHz	5GHz	6GHz	UWB	3GHz	4GHz	5GHz	6GHz	UWB	3GHz	4GHz	5GHz	6GHz	UWB
Chest	waist	62.2	61.5	62.4	58.9	50.4	48.9	48.6	54.8	52.3	54.9	55.5	55.1	58.6	55.6	52.6
	left wrist	58.0	61.3	61.1	62.8	48.7	56.7	52.9	59.2	61.4	51.6	57.4	57.1	60.1	62.1	50.2
	right wrist	57.6	56.9	57.4	59.4	49.8	50.8	51.4	54.9	54.7	43.9	54.2	54.1	56.1	57.0	46.9
	left ankle	65.2	61.6	53.0	56.4	58.4	56.4	60.9	68.8	66.1	50.8	60.8	61.2	60.9	61.3	54.6
	right bicep	56.0	61.7	63.3	61.2	55.4	61.0	58.5	59.2	62.3	56.5	58.5	60.1	61.3	61.7	55.9
Waist	chest	62.2	61.5	62.4	58.9	50.4	48.9	48.6	54.8	52.3	54.9	55.5	55.1	58.6	55.6	52.6
	left wrist	54.0	53.3	57.4	60.6	57.2	60.9	57.9	60.6	60.9	55.6	57.4	55.6	59.0	60.8	56.4
	right wrist	51.0	54.5	53.4	50.9	50.2	49.6	50.4	51.7	57.0	56.7	50.3	52.4	52.5	54.0	53.4
	left ankle	59.8	55.9	53.9	56.0	57.8	57.7	59.4	59.3	64.9	58.9	58.7	57.7	56.6	60.5	58.4
	right becep	47.7	58.0	55.3	55.1	50.3	59.9	53.6	57.7	58.0	57.0	53.8	55.8	56.5	56.5	54.2
Left wrist	chest	58.0	61.3	61.1	62.8	48.7	56.7	52.9	59.2	61.4	51.6	57.4	57.1	60.1	62.1	50.2
	waist	54.0	53.3	57.4	60.6	57.2	60.9	57.9	60.6	60.9	55.6	57.4	55.6	59.0	60.8	56.4
	right wrist	58.3	62.0	64.1	63.9	53.3	54.2	58.8	59.6	61.4	52.6	56.2	60.4	61.8	62.6	52.9
	left ankle	65.9	66.5	68.3	67.5	63.2	62.4	66.8	67.9	67.6	56.6	64.2	66.6	68.1	67.5	59.9
	right bicep	58.8	61.5	60.7	62.4	56.8	62.3	63.9	64.8	61.7	52.3	60.6	62.7	62.7	62.1	53.1
right wrist	chest	57.6	56.9	57.4	59.4	49.8	50.8	51.4	54.9	54.7	43.9	54.2	54.1	56.1	57.0	46.9
	waist	51.0	54.5	53.4	50.9	50.2	49.6	50.4	51.7	57.0	56.7	50.3	52.4	52.5	54.0	53.4
	left wrist	58.3	62.0	64.1	63.9	53.3	54.2	58.8	59.6	61.4	52.6	56.2	60.4	61.8	62.6	52.9
	left ankle	68.3	65.6	68.1	66.5	56.0	62.5	61.1	64.5	63.6	65.5	65.4	63.4	66.3	65.1	60.7
	right bicep	59.9	61.4	63.3	56.5	60.1	58.0	63.2	63.1	58.2	57.6	58.9	62.3	63.2	57.4	58.9
left ankle	chest	65.2	61.6	53.0	56.4	58.4	56.4	60.9	68.8	66.1	50.8	60.8	61.2	60.9	61.3	54.6
	waist	59.8	55.9	53.9	56.0	57.8	57.7	59.4	59.3	64.9	58.9	58.7	57.7	56.6	60.5	58.4
	left wrist	65.9	66.5	68.3	67.5	63.2	62.4	66.8	67.9	67.6	56.6	64.2	66.6	68.1	67.5	59.9
	right wrist	68.3	65.6	68.1	66.5	56.0	62.5	61.1	64.5	63.6	65.5	65.4	63.4	66.3	65.1	60.7
	right bicep	66.4	67.6	66.1	67.3	64.9	63.8	66.0	68.0	67.1	61.4	65.1	66.8	67.0	67.2	63.2
right bicep	chest	56.0	61.7	63.3	61.2	55.4	61.0	58.5	59.2	62.3	56.5	58.5	60.1	61.3	61.7	55.9
	waist	47.7	58.0	55.3	55.1	50.2	59.9	53.6	57.7	58.0	57.0	53.8	55.8	56.5	56.5	53.2
	left wrist	58.8	61.5	60.7	62.4	56.8	62.3	63.9	64.8	61.7	52.3	60.6	62.7	62.7	62.1	53.1
	right wrist	59.9	61.4	63.3	56.5	60.1	58.0	63.2	63.1	58.2	57.6	58.9	62.3	63.2	57.4	58.9
	left ankle	66.4	67.6	66.1	67.3	64.9	63.8	66.0	68.0	67.1	61.4	65.1	66.8	67.0	67.2	63.2

application to the body. Figures 5a and 5b demonstrate how increasing the bend severity (i.e. reducing bend radius) generally results in a larger power loss across both isolated and body-worn scenarios for all narrowband and UWB tests. The figures also demonstrate how bending of the antenna has less impact for wearable scenarios compared to that of the isolated. Bending also generally has less effect on the higher frequencies, with bending the antenna on the body at 6 GHz yielding an increase compared to the flat antenna. For the body-mounted antenna (case of most interest) the mean power differences compared to the unbent antenna scenario are -4.6 dB, -4.3 dB, -6.4 dB, +2.0 dB, and -3.3 dB for 3/4/5/6 GHz and UWB frequency bands respectively.

With regards to application of the antennas to the selected medical body parts, the chest and waist have a low antenna bend radii due to being appended to a comparably flat surface, whereas the antennas on the bicep, wrists and ankle have higher bend radii due to the physical attributes of the body. Bend radii are 350mm, 45mm, 55mm, and 28mm for the waist, wrist, bicep, and ankle respectively, and in excess of 600mm (and slightly concave) for the chest. It is noted that the ankle has the largest bending (smallest radius)

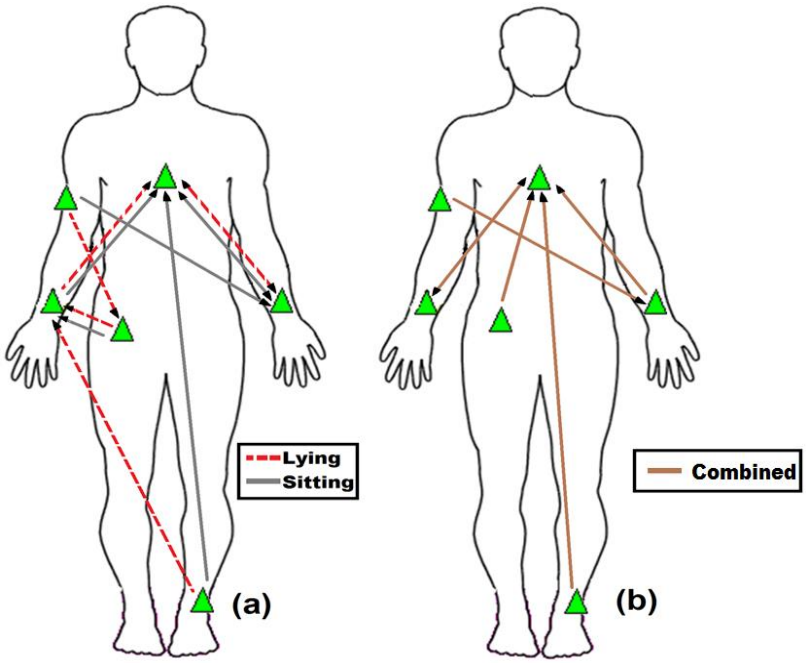

Fig. 6. *UWB highest power links derived from the most frequently occurring highest link power*
a) UWB highest power links for separate lying and sitting postures.
b) UWB highest power links for postures combined.

and is also the furthest away from the others, explaining why the various links to the ankle have the highest path losses (Table 1).
Additionally it is also necessary to consider the polarisation properties of the antennas when mounted upon a body, as the antenna's electric field polarised perpendicular to surface of the human body is propagating along the body with less attenuation compared to the case of electric field polarised parallel to surface of the human body. This also means that results for isolated antennas and off-body scenarios are not applicable to this study.

3.2. *Analysis of Link Powers for Point-to-point Links*

We investigated the link powers between each node within the hospital environment for a single hop point-to-point link. We analyzed each node in turn and observed the statistical mean received power from each of the other network nodes. The various combinations and permutations are displayed in Table 1 as node-to-node path loss values.

3.2.1 UWB: Analysing the results (Table 1) for the lying and sitting postures individually, it was observed that the chest node had the best average link power from all the other nodes for the lying position, and the same was true for the sitting position. Studying the combined results for the lying and sitting postures together revealed that the chest node (highest bend radius) had the best average link power from the other nodes. This suggests that the chest is the optimal location for a master node. This is clearly supported by the pictorial representation of statistical analysis of the most frequently occurring links to nodes with the highest link powers (Fig. 6a and Fig. 6b) and suggests that these nodes should typically be allocated significant processing power and memory to ensure best routing of medical data or the best nodes to facilitate distributed computing activities.

3.2.2 Narrowband: For the lying position the waist node consistently had the best average link power from all other nodes for 3, 4, 5, and 6 GHz operating frequencies (Table 1). For the sitting position the same was found to be true across all four narrowband frequencies. The ankle had the lowest average received power across all frequencies for both sitting and lying positions. For combined posture results the waist node had the highest average link power from all other nodes for all frequencies, and the ankle had the lowest received power across all frequencies. This is summarised in Fig. 7a-c based on a statistical survey of the links with the most frequently occurring highest link power and underscores the waist as the node with highest link power for many of the on-body links. The waist had the second largest antenna bend radius which would support the results presented in Fig. 5 which correlates less antenna bending with higher link power.

3.2.3 UWB and Narrowband comparison: For each link combination we selected the lowest path loss values for the 4 narrowband results and compared them to the UWB result in an effort to understand which scheme offers less path loss; results are presented in Fig. 8 along with the aggregated measurement variations (± 3 standard deviations) of the sample sets for each frequency and posture. UWB consistently had lowest path loss compared to all the narrowband frequencies when averaged across all node-to-node links studied (Fig. 8). It was also discovered that UWB has less path loss than the narrowband equivalent in 63% of the link combinations for the lying position and 67% for the sitting position (derived from data in Table 1). Thus it can be concluded that UWB experiences less on-body path loss than the narrowband equivalent. It is considered that the reason for this lies in UWB being significantly more robust to multipath with the value of path loss exponents typically being higher for narrowband compared to UWB [34].

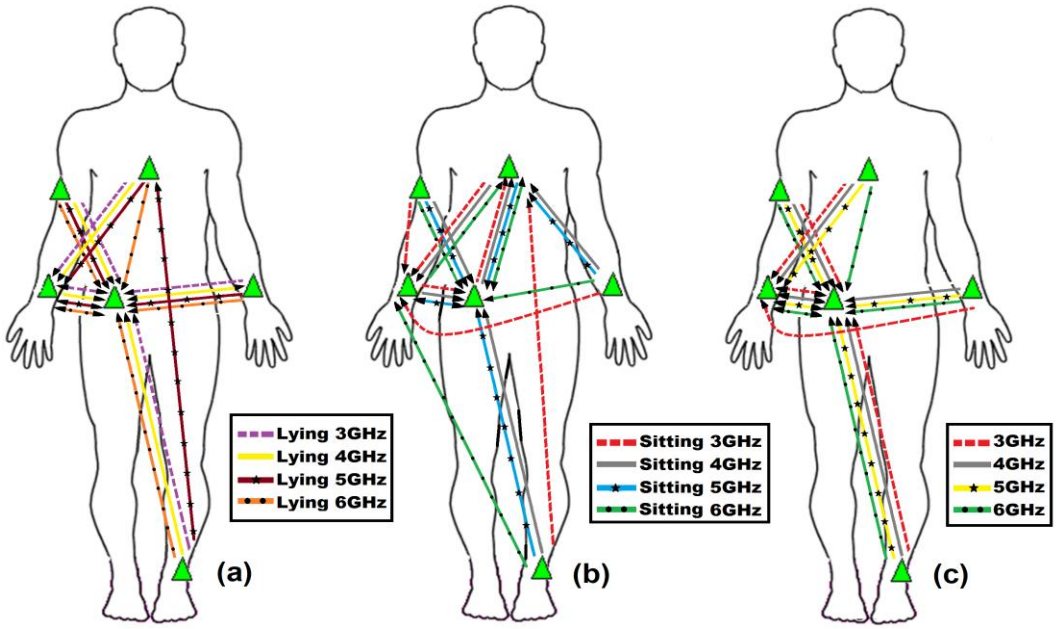

Fig. 7. *Narrowband highest power links derived from the most frequently occurring highest link power*
a) Separate lying posture.
b) Separate sitting posture.
c) Combined postures.

3.3. *Analysis of Link Powers for a Medical Mesh Network*

The previous section assumes a point-to-point star topology; however mesh topologies are employed for network arrangement to offer link redundancy and raise link robustness in a changing modern hospital environment. We thus analyse best route selections for a multi-hop mesh network topology by studying the path loss from each of the various combinations within the mesh network to understand which links would benefit from use of multi-hop strategies in transmitting the data. This is the basis for an opportunistic network where each node routes through the highest power link. For example, for the bicep to chest link for lying UWB, using opportunistic best power links the data can make 3 hops link (bicep to waist to right wrist to chest) instead of using the direct which yields a 5.2 dB benefit. Likewise, for the left wrist to chest link for sitting posture at 3 GHz, the data can make 3 hops (left wrist to right wrist to waist to chest) instead of using the direct which yields a 2.5 dB benefit. In practical terms this may reduce error rates, dropped links, and offer a more robust system. While most previous work highlighted point-to-point links [4, 5, 7] it is advantageous to realize a body-area mesh network in less favourable environments to incorporate inherent robustness and link redundancy.

3.3.1 UWB: Fig. 6 depicts the links with highest received signal strength and suggests best routes for a mesh network topology. Fig. 6a shows the UWB highest power links for separate lying and sitting postures, while Fig. 6b shows UWB highest power links for both postures combined. For example, in the scenario for the lying and sitting postures combined (Fig. 6b) the best route to ensure robust data links from the right bicep to the waist is not a direct link; instead it is from the bicep to the left wrist, then to the chest, then from the chest to the waist. Fig. 6a and Fig. 6b show that for both the separate postures and combined postures, the chest is the main node through which most data routes, and thus is the node that would route the majority of data around the UWB system. In practical terms this may signify that this node should be allocated the most processing power and memory.

3.3.2 Narrowband: Fig. 7a-7c display the links with the highest received signal strength and as before can be studied to reveal the best routes around the narrowband body area network. Most of the best links are through the waist, e.g., ankle to bicep is from ankle to waist, then waist to bicep. The lying position (Fig. 7a) strongly favours the waist and right wrist as nodes to route through, while the sitting position (Fig. 7b) increases the importance of the chest node. The combined overall results (Fig. 7c) show the waist and right wrist as key routing nodes. Overall, the ankle and

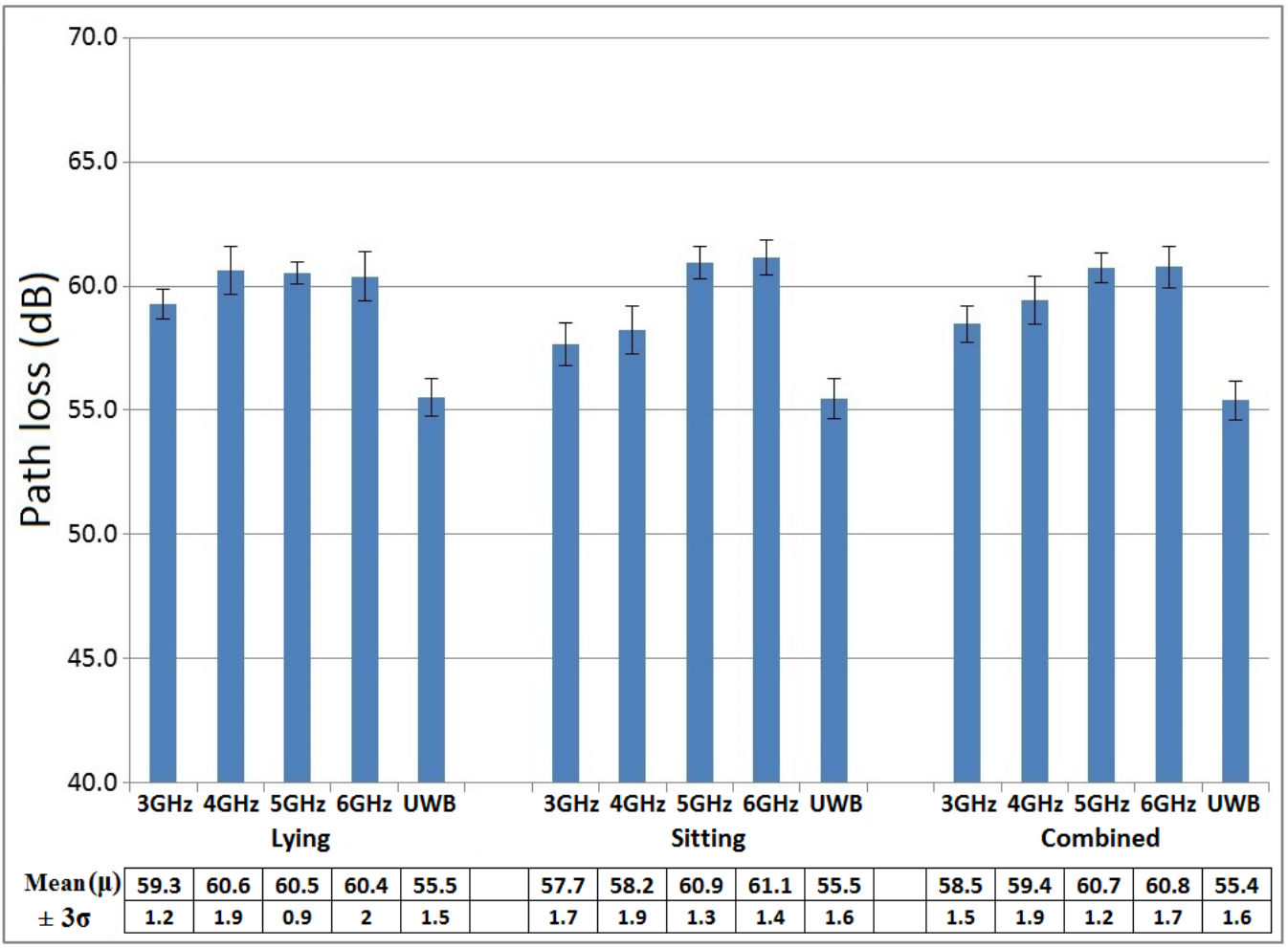

Mean (μ)	59.3	60.6	60.5	60.4	55.5		57.7	58.2	60.9	61.1	55.5		58.5	59.4	60.7	60.8	55.4
± 3σ	1.2	1.9	0.9	2	1.5		1.7	1.9	1.3	1.4	1.6		1.5	1.9	1.2	1.7	1.6

Fig. 8. *Mean path loss over all links arranged by frequency band and posture, with ± 3σ sample variation bars*

bicep were never the highest power links and the left wrist rarely. The nodes on the extremities are therefore better routed through the waist/right wrist to other nodes to ensure every node can robustly link with all other nodes in the mesh network.

3.3.3 UWB and narrowband comparison: It was noted that there appears to be generally less hops to navigate the highest power links in narrowband compared to UWB, particularly from extremities. This can be attributed to UWB being more robust to multipath with higher path loss exponents for narrowband compared to UWB observed by [34].

4. Conclusions

This paper has presented results from an experimental campaign to understand the requirements for future medical body-area networks in a hospital ward environment and directly compares link quality for 4 narrowband operating frequencies (3, 4, 5, and 6 GHz) as well as for UWB. This work demonstrates the genuine potential to realise wireless mesh whole-body healthcare monitoring in a hospital setting. The flexible antenna bend radius and body location is considered to strongly influence link path loss, with small bend radii unavoidable on certain bodily surfaces; also the polarisation properties of the antennas when mounted upon a body have a marked effect on the performance of the body area network links with the antenna's electric field polarised perpendicular to surface of the human body is propagating along the body experiencing less attenuation than the electric field polarised parallel to surface of the human body.

The most suitable body locations for a master processing and routing node (point-to-point link from other nodes) shows how the best node may vary depending on the patient's posture and frequency scheme used; in practice this may suggest a distributed computing scheme is beneficial. For the UWB network it was observed that the chest node had the best average link power from all the other nodes for the lying position, the sitting position, and the combined postures together. For the narrowband networks, the waist node consistently had the best average link power from all the other nodes for all operating frequencies for lying and sitting positions, and also for the combined results of lying and sitting. This can be used to inform system designers regarding which areas of the medical body area network require more processing power, increased launch power, and better development of antenna design to facilitate nodes on the extremities.

Best route selections for multi-hop mesh network topologies were discussed to establish a better understanding of what strategies may be used to ensure highly robust whole-body medical networks. It is recognised that there is a balance required between the node processing power needed to facilitate serial multi-hops between nodes and the value of passing data between the node-to-node link with the best RSSI. To this end, future work will include developing learning algorithms and models which help establish the optimal hopping strategy for a particular network wearer, as well as for particular selection of sensors (for example, if monitoring ankle-brachial index is not necessary then the patient's network will not necessarily have an ankle sensor node). For the UWB network the chest was the main node through which most data connects for each posture, and is thus the node through which data from extremities should be routed. For each of the narrowband networks the lying position strongly favoured the waist and right wrist as key route nodes, while the sitting position favoured the chest node. For combined posture results the waist and right wrist were the key routing nodes, and thus data from extremities are better routed through the waist/right wrist node. Understanding this is important for transmitting data from sensors on extremities to other sensors on extremities as the direct links often have low power and thus multi-hop strategies offer more robust links. These results will inform development work into emerging next-generation wearable hospital monitoring solutions that embrace whole-body mesh networking strategies and help designers develop optimal antenna design for specific body parts including better directionality of certain antennas to increase both individual link robustness as well as overall system robustness.

5. References

[1] Lubecke, V.: 'Wearable wireless electronics'. IEEE MTT-S Intl. Microwave Symp. (IMS), USA, 2015, pp.1-4.

[2] Zhi Hao, J., Brocker, D.E., Sieber, P.E., *et al.:* 'A Compact, Low-Profile Metasurface-Enabled Antenna for Wearable Medical Body-Area Network Devices', IEEE Trans. Ant. and Prop., **62,** (8), Aug. 2014, pp.4021-4030.

[3] Hamalainen, M., Kumpuniemi, T., Iinatti, J.: 'Observations from ultra wideband on-body radio channel measurements'. General Assembly and Scientific Symposium 31st URSI, 2014, pp.1-4.

[4] Chen, X. Lu, X., Jin, D., *et al.:* 'Channel Modeling of UWB-Based Wireless Body Area Networks'. IEEE Int. Conf. on Communications (ICC), 2011, pp.1-5.

[5] Kim, J-W., Kim, Y., Kim, S. C.: 'Ultra WideBand Channel Characteristics for Body Area Network'. 2014 IEEE 79th Veh. Tech. Conf. (VTC Spring), 2014, pp.1-5.

[6] Khan, M.M.: 'Comparison of narrowband and ultra wideband subject-specific on-body radio channel studies for healthcare applications'. 2nd Int. Conf. Green En. Tech. (ICGET), 2014, pp.139-144.

[7] Hu, Z., Nechayev, Y., Hall, P.S., *et al.:* 'Measurements and statistical analysis of on-body channel fading at 2.45 GHz', IEEE Ant. Wire. Prop. Lett., **6**, 2007, pp.612- 615.

[8] Smith, D.B., Miniutti, D., Hanlen, L.W.: 'Characterization of the Body-Area Propagation Channel for Monitoring a Subject Sleeping', IEEE Trans. Ant. Prop., **59**, (11), Nov. 2011, pp.4388-4392.

[9] Donnelly, N., Hunniford, T., Harper, R., *et al.:* 'Demonstrating the accuracy of an in-hospital ambulatory patient monitoring solution in measuring respiratory rate'. IEEE EMBS 35th Ann. Int. Conf., Japan, July 3-7 2013, pp.6711-6715.

[10] Schreiner, C., Catherwood, P., Anderson, J., *et al.:* 'Blood oxygen level measurement with a chest-based pulse oximetry prototype system'. Comp. in Cardio., Belfast, UK, 2010, pp.537-540.

[11] Salman, S., Wang, Z., Colebeck, E., *et al.:* 'Pulmonary Edema Monitoring Sensor With Integrated Body-Area Network for Remote Medical Sensing', IEEE Trans. Ant. and Prop., **62**, (5), May 2014, pp.2787-2794.

[12] Lynn, W., Escalona, O., McEneaney, D.: 'Approaching Long Term Cardiac Rhythm Monitoring Using Advanced Arm Worn Sensors and ECG Recovery Techniques', Intl. Journal Cardiology and Angiology, **3**, (3), 2015, pp.137-148.

[13] Nelson, M.R., Quinn, S., Winzenberg, T.M., et al.: 'Ankle-Brachial Index determination and peripheral arterial disease diagnosis by an oscillometric blood pressure device in primary care', BMJ Open, **2**, (5), 2012.

[14] Lauzier, M., Ferrand, P., Fraboulet, A., et al.: 'Full mesh channel measurements on Body Area Networks under walking scenarios'. 7th Euro. Conf. Ant. Prop. (EuCAP), 2013, pp.3508-3512.

[15] Bykowski, M., Tracey, D., Graham, B., et al.: 'A schema for the selection of network topology for Wireless Body Area Networks'. IEEE Radio Wireless Symp., 16-19 Jan. 2011, pp. 390-393.

[16] D'Errico, R., Rosini R., Maman, M.: 'A Performance Evaluation of Cooperative Schemes for On-Body Area Networks Based on Measured Time-Variant Channels'. 2011 IEEE Intl. Conf. on Comms. 2011, pp. 1-5.

[17] Gorce, J.M., Goursaud, C., Villemaud, G., D'Errico R., Ouvry, L.: 'Opportunistic relaying protocols for human monitoring in BAN'. 2009 IEEE 20th Intl. Symp. Personal, Indoor and Mobile Radio Comms. 2009, pp. 732-736.

[18] Hamida, E.B., D'Errico R., Denis, B.: 'Topology Dynamics and Network Architecture Performance in Wireless Body Sensor Networks'. 2011 4th IFIP Intl. Conf. on New Tech., Mobility and Security. 2011, pp. 1-6.

[19] Natarajan, A., de Silva, B., Yap K.K., Motani, M.: 'To Hop or Not to Hop: Network Architecture for Body Sensor Networks'. 6th Ann. IEEE Comms. Soc. Conf. Sensor, Mesh and Ad Hoc Comms. and Net.. 2009, pp. 1-9.

[20] Maman, M., Mani, F., Denis B., D'Errico, R.: 'Evaluation of multiple coexisting Body Area Networks based on realistic on-body and Body-to-Body channel models'. Intl. Symp. Med. Info. Comm. Tech. 2016, pp. 1-5.

[21] Boeykens, F., Vallozzi, L., Rogier, H.: 'Cylindrical Bending of Deformable Textile Rectangular Patch Antennas', Int. J. Ant. Prop., ID 170420, 2012, pp.1-11.

[22] Abbasi, Q.H., Rehman, M.U., Yang, X., et al.: 'Ultrawideband Band-Notched Flexible Antenna for Wearable Applications', IEEE Ant. Wirel. Prop. Lett., **12**, 2013, pp.1606-1609.

[23] Catherwood, P.A., Scanlon, W.G.: 'Body-centric ultra-wideband multichannel characterisation and spatial diversity in the indoor environment', IET Micr. Ant. & Prop., **7**, (1), 2013, pp.61-70.

[24] Liang, X.L.: 'Ultra-Wideband Antenna and Design, Ultra Wideband - Current Status and Future Trends'. M. Matin (Ed.), InTech, 2012.

[25] Haraz, O., Sebak A.R., 'UWB Antennas for Wireless Applications, Advancement in Microstrip Antennas with Recent Applications'. Prof. A. Kishk (Ed.), InTech, 2013.

[26] A. Paraskevopoulos, D. d. S. Fonseca, R. D. Seager, W. G. Whittow, J. C. Vardaxoglou and A. A. Alexandridis, "Higher-mode textile patch antenna with embroidered vias for on-body communication," *in* IET Microwaves, Antennas & Propagation, vol. 10, no. 7, pp. 802-807, 5 15 2016.

[27] Scanlon, W.G., Cotton, S.L.: 'Understanding on-body fading channels at 2.45 GHz using measurements based on user state and environment'. Loughborough Ant. Prop. Conf., 2008, pp. 10-13.

[28] D'Errico, R., Ouvry, L.: 'Time-variant BAN channel characterization'. IEEE 20th International Symp. Personal, Indoor and Mobile Radio Comms., 2009, pp. 3000-3004.

[29] Abbasi, Q,H., Sani, A., Alomainy, A., *et al.:* 'Numerical Characterization and Modeling of Subject-Specific Ultrawideband Body-Centric Radio Channels and Systems for Healthcare Applications', IEEE Trans. on Info. Tech. in Biomedicine, **16**, (2), March 2012, pp.221-227.

[30] Di Franco, F., Tachtatzis, C., Graham, B., *et al.:* 'The effect of body shape and gender on wireless Body Area Network on-body channels'. 2010 IEEE Middle East Conf. on Ant. and Prop. (MECAP), 2010, pp.1-3.

[31] Sani, A., Alomainy, A., Palikaras, G., *et al.:* 'Experimental Characterization of UWB On-Body Radio Channel in Indoor Environment Considering Different Antennas', IEEE Trans. Ant. and Prop., **58**, (1), Jan. 2010, pp.238-241.

[32] Michalopoulou, A., Alexandridis, A.A., Peppas, K., *et. al.:* 'Statistical Analysis for On-Body Spatial Diversity Communications at 2.45 GHz', IEEE Trans. Ant. and Prop., **60**, (8), Aug. 2012, pp.4014-4019.

[33] van Roy, S., Quicois, F., Liu, L., *et al.:* 'Dynamic Channel Modeling for Multi-Sensor Body Area Networks', IEEE Trans. Ant. Prop., **61**, (4), Apr. 2013, pp.2200-2208.

[34] Khan, M.M.; 'Comparison of narrowband and ultra wideband subject-specific on-body radio channel studies for healthcare applications', Intl. Conf. Green Energy and Technology, 2014, pp.139-144.